https://doi.org/10.5194/tc-2020-56
Preprint. Discussion started: 3 May 2020

The Cryosphere Discussions
Open Access

Liquid-water content and water distribution of wet snow using electrical monitoring.

Pirmin Philipp Ebner[1], Aaron Coulin[1], Joël Borner[1], Fabian Wolfsperger[1], Michael Hohl[1], Martin Schneebeli[1]

[1] WSL Institute for Snow and Avalanche Research SLF, Davos Dorf, 7260, Switzerland

Correspondence to: Martin Schneebeli (schneebeli@slf.ch)

Abstract:

Snow exists in a wide range of temperatures and around its melting point snow becomes a three-phase material. A better understanding of wet snow and the first starting point of water percolation in the seasonal snowpack is essential for snow pack stability, snow melt run-off and remote sensing. In order to induce and measure precisely the liquid water and the corresponding dielectric properties inside a snow sample, an experimental setup was developed. Using microwave heating at 18 kHz allows the use of dielectric properties of ice to enable heat to be dissipated homogeneously through the entire volume of snow. A desired liquid water content inside the snow sample could then be created and analysed in a micro-computer tomography. Based on the electrical monitoring a promising perspective for retrieving water content and water distribution in the snowpack is given. The heating process and extraction of water content are mainly dependent on the morphological properties of snow, the temperature and the liquid water content. The experimental observation can be divided in three different heating processes affecting the dielectric properties of snow for different densities: (1) dry snow heating process up to 0 °C indicating a temperature and snow structure dependency of the dielectric property of snow; (2) wet snow heating at stagnating temperature of 0°C and the presence of uniformed distributed liquid water changes the dielectric properties. The presence of liquid water decreases the impedance of the snow sample until water starts to percolate; and (3) the start of water percolation is between 5-12 water volume fraction depending on the

https://doi.org/10.5194/tc-2020-56
Preprint. Discussion started: 3 May 2020

snow density and confirms the literature findings. The onset of water percolation initiated an inhomogeneity in snow and water distribution, strongly affecting the dielectric properties of the snow. These findings are pertinent to the interpretation of the snow melt run-off of spring snow. These laboratory measurements allow to find the narrow range of the starting point of water percolation in coarse-grained snow and to extract the corresponding dielectric properties which is important for remote sensing.

https://doi.org/10.5194/tc-2020-56
Preprint. Discussion started: 3 May 2020

The Cryosphere Discussions
Open Access

1. Introduction

Snow, a sintered porous material made of ice grains, has a complex porous microstructure and consist of a continuous ice structure at temperature below zero degrees (Löwe et al., 2011). Reaching the melting point, snow becomes a three-component mixture of ice, water and air. A detailed understanding of the influence of liquid water on the snow microstructure is essential. It influences radar and microwave attenuation, sub-surface exploration, remote sensing, radar altimetry, electrical grounding, atmospheric electrical fields and electrostatic charging by precipitation and blown particles (Mellor, 1977). Liquid water in snow is also a critical factor for estimating the hazard of wet snow avalanches and the transmission of melt-water through a snow-pack (Evans, 1965; Reiweger et al., 2015).

Estimating liquid water content is difficult even for experienced observers (Martinec, 1991; Fierz and Föhn, 1994), partly because water flow through snow varies both spatially and temporally (e.g. Colbeck 1979; Marsh, 1988; Conway and Benedict, 1994). Introduction of liquid water into snow changes morphological (Brun, 1989; Coléou and Lesaffre, 1998; Raymond and Tusima, 1979; Brun, 1989; Marsh, 1987; Colbeck, 1997; Marshall et al., 1999; Jordan et al., 2008) and mechanical properties of snow (Techel et al., 2011; Colbeck, 1982). When liquid water occurs for the first time in the seasonal snowpack, much water can be hold as small grains cause high capillary forces. After a couple of melt-freeze cycles smaller grains disappear and less melt-water is held immobile in the snow matrix (Yamaguchi et al., 2010). This delays water runoff during the early stages of snowpack melt-out and snow can retain liquid water (Colbeck, 1972; Linsley et al, 1949). Reaching a saturation point, the liquid water is then released suddenly. The transition point where the liquid water starts to percolate in the snow sample is important because it dominates the spring runoff period in many regions.

Measuring the liquid water content non-destructively and homogeneously in larger snow samples (in centimetre regime) is very challenging. The small amount of liquid water present and the sensitivity of the snow to the various processes to induce a defined liquid water content makes the measurements hard. Radiative absorption or snow melting in a room at 0°C induces a temperature gradient from the surface to the core of the snow sample leading to an inhomogeneous liquid-water content

https://doi.org/10.5194/tc-2020-56
Preprint. Discussion started: 3 May 2020

distribution. The direct supply of liquid water causes percolation in preferential selected channels. In both cases, the water distribution is not homogeneous and the exact extraction of the starting point of water percolation is not possible. In contrast, Coléou and Lesaffre (1998) performed experiments by slowly saturate a snow sample fully with water and afterwards drained out to find the starting point of water percolation. They approached the water retention curve of snow (Yamaguchi et al., 2010) from the right site. In these experiments water percolation was initiated at around 5-14 % of mass volume for snow density between 350 kg m^{-3} and 680 kg m^{-3} (Coléou and Lesaffre, 1998).

Another way to induce a homogeneous liquid-water content into the snow without destroying the snow sample is microwave heating (Brun, 1989; Camp and LaBrecque, 1992). In this case, the water retention curve of snow (Yamaguchi et al., 2010) is approached from the left site. A uniform electric field oscillating at an appropriate frequency excites the dielectric properties of ice enabling heat to be dissipated through the whole volume of snow (Mellor, 1977; Brun, 1989; Camp and LaBrecque, 1992). The dielectric properties of the ice depend on the frequency, temperature and snow density. The applied field results in a displacement of charged particles in the insulating material, giving rise to induced dipoles. The permanent dipoles of the water molecule respond to the electric field, which results in a temperature increase of the material. The heat absorption by the ice phase is uniform and the absorbed energy depends only on the imaginary part ε'' of permittivity (Polder and Van Santen, 1946).

Dielectric properties of dry snow are closely related to solid ice. The ideal relaxation-frequency of ice is at 7.5 kHz (Auty and Cole, 1952). However, the relaxation frequency of dry snow lies between 10 and 100 kHz depending on the snow density and temperature (Bader and Kuroiwa, 1962; Polder and Van Santen, 1946; Evans, 1965). The presence of liquid water strongly affects the dielectric properties of the wet snow sample (Sweeny and Colbeck, 1974; Ambach and Denoth, 1980, Camp and LaBrecque, 1992). A wide spectrum of frequencies has been explored to determine the free water content of water in snow (Ambach and Denoth, 1975; Boyne and Fisk, 1987; Brun, 1989; Denoth et al., 1984; Denoth and Foglar, 1986; Perla, 1990; Camp and LaBrecque, 1992). As long as the liquid water phase remains discontinuous on the ice matrix (Brun E., 1989), the dielectric properties of the wet snow sample are homogenous over the whole sample and the amount of liquid water can be estimated (Ambach and Denoth, 1972, Koch et al., 2014). At the point where the liquid water starts to percolate, an inhomogeneous distribution of water and ice starts to build up in the total snow sample and locally affects the dielectric properties of the sample. Work by Camp and LaBrecque (1992) showed that dielectric heating at 20 kHz is a useful means of modifying the water content from 0 to 30% by weight.

The objective of this paper is to present an experimental setup to allow standardized studies to extract the starting point of water percolation depending on snow density and dielectric properties. We developed a dielectric heating device at 18 kHz, similar to the work by Brun (1989) and Camp and LaBrecque (1992), to find the narrow range of the starting point of water percolation in coarse-grained snow. We improved the suggested power measurements by improving the measurement of phase to be more sensitive in the control of water content. Our technique of monitoring the voltage, current and phase shift at the two copper plates makes it possible to study the dielectric properties of the snow as the water content changes. In particular, at temperature close to the melting point the surface properties of the ice change markedly affecting the dielectric properties. Additionally, with the well-controlled electrical heating the exact water content of water percolation of different kind of snow densities and surface-to-volume ratio can be extracted. We analysed three regimes: (1) dry snow heating showing the fraction of energy absorption of the snow, (2) producing wet snow to investigate the starting point of water percolation based on the electrical properties and density of the snow. Additionally, primarily quantifying of the water content in three-dimensional space without destroying the snow structure are analyzed using micro computed tomography (micro-CT); (3) water percolation affecting the overall impedance of the snow sample.

2. Experimental setup

The experimental setup is shown schematically in Fig. 1 and a photo of the experimental setup is shown in Fig. 2. The device consists of three functional blocks: (1) low voltage circuit to generate the sinusoidal signal and amplify the energy output, (2) high voltage circuit to transform the low primary voltage to a high secondary voltage, and (3) design of the sample holder between the high voltage capacitor plates.

https://doi.org/10.5194/tc-2020-56
Preprint. Discussion started: 3 May 2020

The core of the snow heater is a Red Pitaya STEM 125-14 using for signal generation and data acquisition, and is controlled via Standard Commands Programmable Instruments SCPI in Matlab. The low voltage sinusoidal input signal with a frequency of 18 kHz is generated by a high-speed digital to analog converter and is amplified afterwards to stabilizes the electrical potential in the circuit. A step-up transformer transforms the low primary voltage to a high secondary voltage of around 350 V applied to two copper plates inducing the dielectric heat into the snow sample. The surface of the copper plates is electrically insulated to prevent Joule heating of the snow sample. The snow sample was placed into a polyoxymethylene (POM) ring (diameter = 60 mm, distance = 13 mm) and inserted between the two capacitor plates. The snow sample and the capacitor are thermally insulated with extruded polystyrene foam (XPS) with a thickness of 120 mm to prevent radial conductive and convective heat losses.

The applied sinusoidal waveforms of voltage U(t) to the copper-plates is attached to a differential probe and is measured galvanic sorted with a 100-fold attenuation. The current I(t) from the plate is measured via a shunt resistor. The phase shift $\varphi(t)$ between the sinusoidal waveforms of voltage and current is measured between the circuit's input and circuit's output signal. An input protection circuit prevent the analog to digital converter from damage in case of a short circuit. The voltage connection between the low and high voltage part is measured via a shunt resistor. This connection defines the star point of the circuit and makes sure that the second part of the circuit doesn't thrift away. It is the only star point preventing the circuit from circular currents. A negative temperature coefficient element is placed one centimetre inside the snow sample to measure the temperature. A low pass filter is applied to block the noise of the capacitor.

The total power P_{RMS}(t) between the two copper-plates is calculated based on the root-mean-squared voltage U_{RMS}(t), current I_{RMS}(t) and the measured phase difference $\varphi(t)$

$$P_{\mathrm{RMS}}(t) = U_{\mathrm{RMS}}(t) \cdot I_{\mathrm{RMS}}(t) \cdot cos\varphi(t) \tag{1}$$

The impedance R_{RMS}(t), describing the resistant of the snow sample, between the two copper-plates is given by

https://doi.org/10.5194/tc-2020-56
Preprint. Discussion started: 3 May 2020

$$R_{RMS}(t) = \frac{U_{\mathrm{RMS}}(t)}{I_{\mathrm{RMS}}(t)} \qquad (1)$$

The uncertainties of the temperature T(t), current I_{RMS}(t), voltage U_{RMS}(t), phase shift φ (t), total power consumed P(t), and density of the snow measured by weighting are: ±0.05 °C, ±0.01 mA, ±0.5 V, ±2 degrees, ±0.005 W and ±20 kg m^{-3}.

2.1 Tomography experiments

A cooled micro-computer tomograph (CT; Scanco Medical μ-CT80) at a cold laboratory temperature of -5 °C was used to visually quantify the water content in three-dimensional space without destroying the snow structure. The scanned image had a volume of 200 x 200 x 20 voxels (3.6 mm x 3.6 mm x 0.36 mm) with a nominal voxel resolution of 18 µm. The grey scale resolution for each voxel was 16 bit and a Gaussian filter (σ = 1.4, support = 3) was applied to reconstruct the micro-CT images. The volume was segmented to a binary image by classifying each voxel by ice or air. The threshold for the segmentation process was chosen such as that the manually measured density did not deviate more than 12 % from the CT-density in the segmentation process (Riche and Schneebeli, 2013). Each scan took around 2.7 h. Absorption by water and ice are almost identical (Lieb-Lappen et al., 2017), and are hardly to separate in the segmentation process. Therefore, the water creation on the snow surface was extracted by superposition of two micro-CT scans. One scan was taken before the heating process and the second one afterwards. Before the second micro-CT scan, the wet snow sample was shock frozen at -30 °C to preserve the snow structure. This allowed us to easily visualize and to extract the water creation on the surface of the ice matrix with an uncertainty of 4 %.

3. Method

The phenomena involved in microwave heating of snow are volumetrically absorption of electromagnetic energy to achieve self-heating uniformly and rapidly, which is characterized by the density of the snow. The dielectric power absorption P is equal to the total power consumed P_{RMS}, given by:

$$P = 2 \cdot \pi \cdot f \cdot E^2 \varepsilon_0 \cdot \varepsilon_s''(f, \rho_s, T_s) \cdot A \cdot d = P_{\mathrm{RMS}} \qquad (3)$$

https://doi.org/10.5194/tc-2020-56
Preprint. Discussion started: 3 May 2020

where f is the frequency, $E = U\,d^{-1}$ the electric field, $\varepsilon_0 = 8.85 \cdot 10^{-12}$ the electric field constant, ε_s'' the imaginary part of the complex dielectric constant of snow, A the capacitors surface area and d the distance between the two copper-plates. Rearranging Eq. (3) the imaginary part of the complex dielectric constant of dry snow is given by

$$\varepsilon_s''(f, \rho_s, T_s) = \frac{P_{\mathrm{RMS}}}{2 \cdot \pi \cdot f \cdot E^2 \cdot \varepsilon_0 \cdot A \cdot d} \tag{4}$$

which depends on the frequency f, snow density ρ_s, and snow temperature T_s.

The heating efficiency is an important factor to evaluate the heating process. It is defined as the ratio of energy absorbed by the heated sample to that radiated from the microwave source [Ali, 2016] given by:

$$\eta = \frac{Q_{\mathrm{setup}} - Q_{\mathrm{sample}}}{Q_{\mathrm{setup}}} = 1 - \frac{m_s c_p (T_1 - T_0)}{\int_0^{t_1} P_{\mathrm{RMS}}(t) dt} \tag{5}$$

where m_s is the mass of the snow sample, c_p the specific heat capacity, T_0 and T_1 the initial temperature and melting temperature at 0 °C, and t_1 the time until temperature reached 0 °C.

The liquid water mass fraction for each timestep t, is calculated by the fraction of the measured dissipated latent heat and total latent heat needed for the phase change:

$$x_{\mathrm{mass}}(t) = \frac{\int_{t_1}^{t} \eta \cdot P_{\mathrm{RMS}}(t) dt}{h_{\mathrm{latent}} m_s} \tag{6}$$

where $h_{\mathrm{latent}} = 334$ kJ kg^{-1} is the latent heat for the phase change from ice to water and t_1 the time step where the snow sample reached 0 °C.

The liquid water volume fraction is given by [Coléou and Lesaffre, 1998]:

$$x_{\mathrm{vol}}(t) = \frac{x_{\mathrm{mass}} \cdot \rho_s}{\rho_i - \rho_s} \cdot \frac{\rho_i / \rho_w}{1 - x_{\mathrm{mass}}} \tag{7}$$

https://doi.org/10.5194/tc-2020-56
Preprint. Discussion started: 3 May 2020

where ρ_s, ρ_i and ρ_w are the snow, ice (917 kg m^{-3}) and water (999.9 kg m^{-3}) density. The uncertainties of x_{mass} and x_{vol} are 10 % due to the uncertainty of the power (±0.005 W) and density measurement (±20 kg m^{-3}).

4. Results

Deionized water with a conductivity of ≈ 0.2 μS cm^{-1} was used to produce natural identical snow (Schleef et al., 2014) in a cold laboratory at -20 °C. The produced snow was sieved into sample holders (mesh size: 2 x 2 mm) and was sintered at a temperature of -2 °C for two to five days to allow the snow crystals to form a uniform grain size. A hydraulic press compressed the snow to densities between 400 and 600 kg m^{-3} to represent snow packs in spring (Bartelt and Lehning, 2002). We analysed in total seven different snow samples.

The measured electrical properties between the two copper-plates were strongly influenced by the temperature, water content, and density of the snow sample. The higher the snow density and the water content in the snow was, the stronger the measured electrical properties were affected, shown in Table 1. Figure 3 shows a typical measured temperature T(t), current I_{RMS}(t), voltage U_{RMS}(t), and phase shift φ(t) profile of a heating process for snow density of (a) 438 kg m^{-3}, (b) 539 kg m^{-3}, (c) 612 kg m^{-3}, and (d) 917 kg m^{-3}. The temperature profile shows the characteristic of the snow heating process increasing from -1 °C up to 0 °C. Afterwards the temperature stagnates at 0 °C and the supplied energy was used for the phase change from ice to liquid water. The current profile has a different behaviour. It shows a slightly linear increase until the snow sample reached a temperature of 0 °C. Afterwards the incline of the current curve further increased reaching the highest current of 1.7 mA, 2.6 mA, 3.8 mA, and 4.3 mA at around 80 min, 60 min, 55 min, and 9 min for snow with densities of 438 kg m^{-3}, 539 kg m^{-3}, 612 kg m^{-3}, and 917 kg m^{-3}. After this maximum the current started to decrease with time. The voltage and phase shift showed a mirror inverted behaviour to the current profile. Both parameters decreased with time and increased afterwards again. At the beginning a phase shift of 55.9°, 52.8°, 50°, and 46.9° were measured with the lowest phase shift of 41.3°, 35.2°, 31.5°, and 22.4° for snow densities of 438 kg m^{-3}, 539 kg m^{-3}, 612 kg m^{-3}, and 917 kg m^{-3}.

The snow temperature, density and water content strongly affected the impedance and the total power consumed by the snow sample. The impedance decreased with increasing temperature, water content, and density, vice versa for the total power consumed, shown in Table 2. Figure 4 shows a typical calculated total power $P_{RMS}(t)$ and impedance $R_{RMS}(t)$ profile compared with the measured temperature profile of a heating process for snow density of (a) 438 kg m^{-3}, (b) 539 kg m^{-3}, (c) 612 kg m^{-3}, and (d) 917 kg m^{-3}. The impedance had the same profile behaviour like the phase shift starting with 368.4 kΩ, 275.5 kΩ, 213.5 kΩ, and 123.1 kΩ reaching a minimum of 197.4 kΩ, 127.3 kΩ, 87.3 kΩ, and 73.5 kΩ after 80 min, 60 min, 55 min, and 9 min for snow density of 438 kg m^{-3}, 539 kg m^{-3}, 612 kg m^{-3}, and 917 kg m^{-3}. The total power consumption profile was mirror inverted. It started with 0.17 W, 0.25 W, 0.33 W, and 0.63 W and reached a maximum of 0.41 W, 0.69 W, 1.04 W, and 1.24 W after 80 min, 60 min, 55 min, and 9 min for snow density of 438 kg m^{-3}, 539 kg m^{-3}, 612 kg m^{-3}, and 917 kg m^{-3}.

The heating efficiency was affected by heat loss at the wall and decreases with higher snow density. The microwave power did not directly penetrate into the snow samples but also through the air space of the pores. As a result, the reflection of microwave power on the interface, which was caused by the relative permittivity mismatch between the air and the sample led to limited heating efficiency. As the frequency of 18 kHz was in the range of the optimal snow heating frequency between 10 and 100 kHz depending on the snow density (Bader and Kuroiwa, 1962; Polder and Van Santen, 1946; Evans, 1965), the efficiency of the heating samples was usually higher for lower density. This effect is confirmed by Fig. 5 showing the heating efficiency and the complex dielectric constant of dry snow at T = 0 °C for various snow sample. The error bars indicate the measured uncertainty of the experimental setup. Ice had the lowest heating efficiency with the highest extracted permittivity value of $\varepsilon_{\mathrm{i}}'' = 30.65$, similar to literature values of $\varepsilon_{\mathrm{i}}'' = 30.93$ at 18 kHz [Fujita et al., 2000].

The start of water percolation was between 5-12 water volume fraction depending on the snow density. Dense snow absorbed more microwave energy leading to higher liquid water content in a snow sample in a short time. The temporal evolution of the liquid water mass and volume fraction based on the measured power for the different snow samples (Fig. 6) increased with time and the influence of snow density was

https://doi.org/10.5194/tc-2020-56
Preprint. Discussion started: 3 May 2020

observed. At the maximum of consumed power $P_{RMS}(t)$ a water mass and volume fraction of 7.1 and 6.1, 6.7 and 8.8, 8.7 and 15.4, and 0.4 and 0 for snow density of (a) 438 kg m^{-3}, (b) 539 kg m^{-3}, (c) 612 kg m^{-3}, and (d) 917 kg m^{-3} was reached. Table 3 shows the estimated water mass and volume fraction and time of the different snow sample at the reversal point of the measured power, indicating the start of water percolation.

The created water led to a stronger rounding of the ice crystals and the effect of fast wet snow metamorphism was observed where a growth in size of snow crystals was identified (Colbeck and Davidson, 1973). Figure 7 shows preferential spots of water accumulation inside the snow structure. Blue indicates the ice structure and orange shows the water part. The snow sample with an initial density of around 682 kg m^{-3} was heated to induce a volume water content of 16 %. A volume water content of around 13.3 % was extracted from the difference in the micro-CT scans before and after the experiments. This rounding effect is also shown in an insight in the snow heating process by a microscopy image illustrated in Fig. 8. The photography on the left shows a snow structure of dry snow before and on the right after the experimental run.

4. Discussion

Our major experimental results are summarized in Fig. 4 and 6, and in Table 2 and 3. The dominant sources of absolute errors in the measurement of the water mass and volume fraction in the snow were the snow density and the inaccuracy in the power measurement. Especially, at snow densities below 450 kg m^{-3} this might cause deviations of ± 1 % in the water mass and volume fraction measurement. However, at higher snow densities the relative errors were considerably less.

The snow structure and the water content had a major impact on the electrical properties showing the same behaviour like in the work of Camp and LeBraque (1992). In both works the electrical power increased with increasing water content and drops at one point again. Based on the findings we divided the heating process in three areas, shown in Fig. 9:

https://doi.org/10.5194/tc-2020-56
Preprint. Discussion started: 3 May 2020

(1) Dry snow: The heating process up to 0 °C indicated a temperature and snow structure dependency on the measured values. As snow temperature reached the melting point, the surface properties of the ice structure changed markedly and affected the electrical properties. The vibration and the mobility of protons enhanced and influenced the electrical conductivity leading to a decrease of the impedance. Further, at higher density the structural connections between ice crystals were less destructed by the pore volumes. This allowed a higher rate of flow of electric charge leading to a higher electric current. Additionally, the electrical potential between the two copper-plates was less affected by the pore volume leading to a more stable voltage and smaller phase shift between voltage and current. As a result, the electrical conductivity increased resulting in a lower impedance and a higher electrical energy transfer.

(2) Wet snow: Snow was becoming a particularly complicated medium because the introduction of liquid water caused rapid changes of the important material properties. The temperature stagnated at 0°C and the presence of uniformed distributed liquid water changed the dielectric properties of the snow sample. Additionally, the liquid water layer at the surface allowed the mobility of protons resulting in stronger rate of flow of electric charge and therefore enhanced the electrical conductivity. This reduced the impedance of the two-phase material significantly leading to a decrease of the impedance and phase shift, and an increase in electric current and power.

(3) Water percolation: The water started to percolate and liquid water accumulated at the bottom of the sample holder. The missing water in the upper part of the sample holder treasured up at the bottom of the sample holder and left empty spots at the top where the density decreased locally. The snow probe was not homogeneous anymore leading to a decrease in the electrical conductivity. As a result, the impedance increased again and the electric power decreased. First camera picture of water percolation after an experimental run is shown in Fig. 10. The sample holder was aligned vertically between the capacitor plates. Water percolated in the upper part of the sample and accumulated at the bottom of the sample holder leading to an inhomogeneous mixture of the sample. This inhomogeneous mixture changed the dielectric properties of the complete sample and affected the heating process. After

https://doi.org/10.5194/tc-2020-56
Preprint. Discussion started: 3 May 2020

this state the relative error of the water mass and volume fraction calculation increased.

Based on the findings, water percolation occurred over a narrow range of values in coarse-grained snow (see Table 3) and was initiated at around 5-8 % of the mass volume (see Table 3). For high snow densities where the surface-to-volume ratios were small, our results were lower than found by Coléou and Lesaffre (1998). Following reasons are: (1) they approached the retention curve of snow (Yamaguchi et al., 2010) from the opposite site and therefore the physical processes were different, (2) they fully saturated the snow sample for about 5 minutes. Therefore, the surface tension of water had an additional effect, like a suction effect, holding more water in the pore space. In our approach water could not be held immobile as the percolation started earlier at the smooth ice surface.

Although the micro-CT measurements (see Fig. 7) showed a snow sample after the water percolation point, still preferential spots of water accumulation inside the snow structure could be seen. Three interesting observations were visible after percolation: (1) No water film around the snow structure but isolated smaller and larger water accumulations were visible indicating that phase change from ice to water were happening on preferential spots on the ice crystal. However, it has to mention that the pixel resolution was too coarse to detect an additional thin water film around the snow structure. The created water led to a stronger rounding of the ice crystals and the dendritic structure further disappeared. Nevertheless, no big change in grain shape was observable due to the high density. (2) The gravity had no influence on the orientation of the accumulated water on the ice crystal. It is apparent that the water was uniformly distributed on the single ice crystals. The water droplets were too small to be distracted by the gravity. (3) Single water accumulation links between single neighbouring ice crystals can be seen. The refreezing of the snow sample after the experiment led to single crystals agglomeration and a growth in size of snow crystals (Colbeck and Davidson, 1973).

The electrical heating procedure developed to incrementally melt snow in order to vary the water content and to analyse the created water non-destructive in a micro-CT worked very well. Improving the experimental setup that the frequency can be increased to the GHz-MHz regime for a short period of time, the exact dielectric snow

https://doi.org/10.5194/tc-2020-56
Preprint. Discussion started: 3 May 2020

property based on the snow morphology and water content can be extracted. This will allow to improve remote sensing and field measurements on the snow-water-equivalent (Ambach and Denoth, 1972, Koch et al., 2014).

5. Summary and Conclusion

We designed, fabricated, and tested an experimental setup for in-situ time-lapse nondestructive investigation of water percolation in snow using the electrical properties of snow. Frequency heating close to the relaxation frequency of ice was applied to slowly increase the water content uniformly in the snow sample until liquid water started to percolate. By measuring the temperature and the applied power, the water content in the snow sample at each timestep was deduced. This new instrument allows to elucidating the starting point of water percolation based on measured electrical and morphological properties of the snow. The setup and the obtained results can be used to precisely forecast the run-off time of different density snowpacks and to investigate the mechanical properties, water movements, surface friction, adhesion, and liquid-water measurements, for wet snow and ice.

The experimental observation showed three different heating processes affecting the dielectric properties of snow for different densities: (1) dry snow heating process up to 0 °C indicating a temperature and snow structure dependency of the dielectric property of snow. At warmer temperature, slightly higher complex dielectric constant were measured having higher discrepancy for more dense snow; (2) wet snow heating at stagnating temperature of 0°C and the presence of uniformed distributed liquid water changes the dielectric properties and therefore reduces the impedance of the two-phase material significantly until the starting point of water percolation; and (3) the start of water percolation is between 5-12 water volume fraction depending on the snow density. After this point the snow sample has an inhomogeneous mixture where liquid water treasures up at the bottom of the sample holder and is leaving bigger pores in the upper part leading to an increase of overall impedance of the snow sample.

Our results and conclusions indicate that there is a need for additional validation. Specially, it would be crucial to not only look at the density but also at the specific surface area of the snow at a given density which also affects the capillary forces and

https://doi.org/10.5194/tc-2020-56
Preprint. Discussion started: 3 May 2020

The Cryosphere Discussions
Open Access

therefore the starting point of water percolation. Ideally, the entire snow sample will be tomographically measured before the experiment to extract the morphological parameters. The primarily micro-computer tomography (CT) result (Fig. 7) shows first promising visualization of the preferred spots of liquid water in three-dimensional space without destroying the snow structure. However, more detailed measurements are needed to make stronger statements about preferential spots of water accumulations inside the snow sample.

Acknowledgments:

The authors thank H. Loewe and B. Walter for the constructive reviews and the modelling support.

https://doi.org/10.5194/tc-2020-56
Preprint. Discussion started: 3 May 2020

The Cryosphere Discussions

References:

Ali I. A.: "Effect of load on the heating efficiency and temperature uniformity in multi-mode cavity applicators", Journal of Microwave Power and Electromagnetic Energy, pp. 123-137, 2016. https://doi.org/10.1080/08327823.2016.1190170

Ambach W. and A. Denoth: "Studies on the dielectric properties of snow", Zeitschrift für Gletscherkunde und Glazialgeologie, pp. 113-123, 1972.

Ambach W. and A. Denoth: "On the dielectric constant of wet snow", Proceedings Snow Mechanics Symposium, IAHS-AISH Publication No 114, 1974.

Ambach W. and A. Denoth: "The dielectric behavior of snow: A study versus liquid water content", NTRS, 1980.

Auty R. P. and R. H. Cole: "Dielectric properties of ice and solid", Journal of Chemical Physics, pp. 1309-1314, 1952.

Bader H. and D. Kuroiwa: "The physics and mechanics of snow as a material", Cold Regions Science and Technology, Sect B., 1962.

Bartelt P. and M. Lehning: "A physical snowpack model for the swiss avalanche warning: Part i: numerical model", Cold Regions Science and Technology, pp. 123-145, 2002.

Boyne H. and D. Fisk: "Comparison of snow cover liquid water measurement techniques", Water Resources Research, pp. 1833-1836, 1987.

Brun E.: "Investigation on wet-snow metamorphism in respect of liquid-water content", Annals of Glaciology, pp. 22-26, 1989.

Evans S.: "Dielectric properties of ice and snow – a review", Journal of Glaciology, pp. 773-792, 1965.

Camp P. R and D. R. LaBrecque: "Determination of the Water Content of Snow by Dielectric Measurements", Cold Regions Research & Engineering Laboratory, pp. 1-39, 1992.

Colbeck S.: "A theory of water percolation in snow", Journal of Glaciology, pp. 369-385, 1972.

Colbeck S.: "The capillary effects on water percolation in homogeneous snow", Journal of Glaciology, pp. 85-97, 1974.

Colbeck S.: "A theory for water flow through a layered snowpack", Water Resources Research, pp. 261-266, 1975.

Colbeck S.: "The Difficulties of Measuring the Water Saturation and Porosity of Snow", Journal of Glaciology, pp. 189-201, 1978.
Colbeck S.: "Water flow through heterogeneous snow", Cold Regions Science Technology, pp. 37-45, 1979.
Colbeck S.: "An overview of Seasonal Snow Metamorphism, Rev. Geophys., 20, pp. 45-61, 1982.
Colbeck S.: "A review of sintering in seasonal snow", US Army Cold Regions Research and Engineering Laboratory Report, pp. 97-100, 1997.
Colbeck S. and G. Davidson: "Water percolation through homogeneous snow", IAHS publication, pp. 242-257, 1973.
Coléou C. and B. Lesaffre: "Irreducible water saturation in snow: experimental results in a cold laboratory", Annals of Glaciology, pp. 64-68, 1998
Conway H. and R. Benedict: "Infiltration of water flow into snow", Water Resource Research, pp. 641-650, 1994.
Denoth A.: "Snow dielectric measurements", Advanced Space Research, pp. 233-243, 1989.
Denoth A., A. Foglar, P. Wieland, C. Mätzler, H. Aebischer, M. Tiuri, and A. Sihvola: "The comparative study of instruments for measuring the liquid water content of snow", Journal of Applied Physics, pp. 2154-2160, 1984.
Fierz, C. and Föhn, P.: "Long-term observation of the water content of an Alpine snowpack", in: Proceedings International Snow Science Workshop 1994 Snowbird, Utah, USA, 117-131, 1994.
Fujita S., Matsuoka T., Ishida T., Matsuoka K. and S. Mae: 'A summary of the complex dielectric permittivity of ice in the megahertz range and its applications for radar sounding of polar ice sheets", Physics of Ice Core Records, Hokkaido University Press, 2000.
Hirashima H., S. Yamaguchi, and T. Katsushima: "A multi-dimensional water transport model to reproduce preferential flow in the snowpack", Cold Region Science Technology, pp. 80-90, 2014.
Illangasekare T. H., R. J. Jr. Walter, M. F. Meier, and W. T. Pfeffer: "Modeling of meltwater percolation in subfreezing snow", Water Resource Research, pp. 1001-1012, 1990.
Jordan R., M. Albert, and E. Brun: "Physical processes within the snow cover and their parametrization", in: Snow and climate: physical processes, surface energy

https://doi.org/10.5194/tc-2020-56
Preprint. Discussion started: 3 May 2020

exchange and modeling, edited by: Armstrong R. and E. Brun, Cambridge University Press, pp. 12-69, 2008.

Kaatze U.: "Complex permittivity of water as a function of frequency and temperature", Journal of Chemical and Engineering Data, pp. 371-374, 1989.

Koch F., M. Prasch, L. Schmid, J. Schweizer, and W. Mauser: "Measuring Snow Liquid Water Content with Low-Cost GPS Receivers", Sensors, pp. 20975-20999, 2014.

Lieb-Lappen R., E. Golden, and R. Obbard: "Metrics for interpreting the microstructure of sea ice using x-ray micro computed tomography", Cold Regions Science and Technology, pp. 24-35, 2017.

Marsh P. and M. Woo: "Meltwater movement in natural heterogeneous snow covers", Water Resources Research, pp. 1710-1716, 1985.

Marsh P.: "Grain growth in a wet Arctic snow cover", Cold Region Science Technology, pp. 23-31, 1987.

Marsh P.: "Flow fingers and ice columns in a cold snowcover", in: Proceedings Western Snow Conference, 18-20 April, 1988, Kalispell, Montana, 105-112, 1988.

Marshall H., H. Conway, and L. Rasmussen: "Snow densification during rain", Cold Region Science Technology, pp. 35-41, 1999.

Martinec J.: "Schneefeuchtigkeit mit dem Denoth-Gerät im Vergleich mit dem Handtest, Messungen 11989, 1990 (Snow wetness with the Denoth-meter in comparison to the hand test, measurements 1989, 1990)", internal report 677 (unpublished), WSL Institute for Snow and Avalanche Research SLF, Davos, 1999b.

Mellor M.: "Engineering properties of snow", Journal of Glaciology, pp. 15-66, 1977.

Löwe H., J. K. Spiegel, M. Schneebeli: "Interfacial and structural relaxations of snow under isothermal conditions, Journal of Glaciology, pp. 499-510, 2011.

Lupi S.: "Fundamentals of Electroheating", Springer, ISBN 978-3-319-46015-4, 2017.

Perla R.: "Real permittivity of snow at 1 MHz and 0°C", Cold Regions Science and Technology, pp. 215-219, 1991.

Polder D. and J. H. van Santeen: "The effective permeability of mixtures of solids", Physica, pp. 257-271, 1946.

https://doi.org/10.5194/tc-2020-56
Preprint. Discussion started: 3 May 2020

Raymond C. and K. Tusima: "Grain coarsening of water saturated snow", Journal of Glaciology, pp. 83-105, 1979.

Reiwegger I., J. Gaume, and J. Schweizer: "A new mixed-mode failure criterion for weak snowpack layers", Geophysical Research Letters, pp. 1427-1432, 2015.

Riche F. and M. Schneebeli: "Thermal conductivity of snow measured by three independent methods and anisotropy considerations", The Cryosphere, pp. 217-227, 2013.

Schleef S., M. Jaggi, H. Löwe, and M. Schneebeli: "An improved machine to produce nature-identical snow in the laboratory", Journal of Glaciology, pp. 94-102, 2014.

Sihvola A., E. Nyfors, and M. Tiuri: "Mixing formulae and experimental results for the dielectric constant of snow", Journal of Glaciology, pp. 163-170, 1985.

Smith J. L.: "Hydrology of warm snowpacks and their effects upon water delivery some new concepts", Advanced Concepts and Techniques in the Study of Snow and Ice Resources", pp. 76-89, 1974.

Sweeny B. D. and S. Colbeck: "Measurements of the Dielectric Properties of Wet Snow Using a Microwave Technique", Cold Regions Science and Technology, Research Report 325, 1974.

Techel F., C. Pielmeier, and M. Schneebeli: "Microstructural resistance of snow following first wetting", Cold Region Science Technology, 65, pp. 382-391, 2001.

Tiuri M., A. Sihvola, E. Nyfors, and M. Hallikaiken: "The complex dielectric constant of snow at microwave frequencies", IEEE Journal of Oceanic Engineering, pp. 377-382, 1984.

Tseng P., T. Illangesakare, and M. Meier: "Modeling of snow melting and uniform wetting from migration in a layered subfreezing snowpack", Water Resource Research, pp. 2363-2376, 1994.

Wever N., C. Fierz, C. Mitterer, H. Hirashima, and M. Lehning: "Solving Richards equation for snow improves snowpack meltwater runoff estimations in detailed multi-layer snowpack model", The Cryosphere, pp. 257-274, 2014.

Yamaguchi S., T. Katsushima, A. Sato, and T. Kumakura: "Water retention curve of snow with different grain sizes", Cold Regions Science and Technology, pp. 87-93, 2010.

https://doi.org/10.5194/tc-2020-56
Preprint. Discussion started: 3 May 2020

The Cryosphere
Discussions
Open Access

Table 1: Density of the snow samples and the corresponding voltage U_{RMS}, current I_{RMS}, and phase shift φ_{RMS} at the start of the experiment (init), reaching 0 °C (dry-wet) and the point where the power is maximum (peak).

Density (kg m^{-3})	U_{RMS} (V)			I_{RMS} (mA)			φ_{RMS} (°)		
	init	dry-wet	peak	init	dry-wet	peak	init	dry-wet	peak
427	325.5	325.6	326.9	0.81	0.82	1.21	57.4	57.3	48.7
438	332.6	327.2	328.0	0.90	0.90	1.66	55.9	55.7	41.4
465	328.0	328.3	328.1	1.14	1.16	1.83	52.2	52.2	40.6
465	329.4	330.1	329.9	1.10	1.13	1.81	52.4	52.1	40.7
539	339.1	329.3	327.8	1.23	1.29	2.58	52.8	51.0	35.2
612	331.3	332.0	327.0	1.55	1.65	3.76	49.5	48.8	31.5
917	336.5	327.9	313.8	2.73	3.41	4.27	46.9	34.5	22.4

Table 2: Density of the snow samples and the corresponding impedance U_{RMS} and power P_{RMS} at the start of the experiment (init), reaching 0 °C (dry-wet) and the point where the power is maximum (peak).

Density (kg m^{-3})	R_{RMS} (kΩ)			P_{RMS} (W)		
	init	dry-wet	peak	init	dry-wet	peak
427	403.4	396.9	269.4	0.14	0.14	0.26
438	368.4	362.0	197.5	0.17	0.17	0.41
465	287.8	282.4	179.2	0.23	0.23	0.46
465	300.4	291.1	182.3	0.22	0.23	0.45
539	275.5	254.8	127.3	0.25	0.27	0.69
612	213.4	213.4	87.3	0.33	0.36	1.04
917	123.1	123.1	73.5	0.63	0.92	1.24

https://doi.org/10.5194/tc-2020-56
Preprint. Discussion started: 3 May 2020

Table 3: Density of the snow samples and the corresponding heating time and the water mass and volume fraction where water starts to percolate.

Density (kg m^{-3})	Heating time (min)	Water mass fraction (%)	Water volume fraction (%)
427	94.5	4.1	3.3
438	81.1	6.4	5.2
465	51.2	4.3	4.1
465	55.2	4.6	4.2
539	58.2	5.8	7.3
612	54.5	7.5	12.9
917	8.79	0.3	0

https://doi.org/10.5194/tc-2020-56
Preprint. Discussion started: 3 May 2020

Figure captions:

Figure 1: The experimental setup consisting of three functional blocks (1) low voltage circuit to generate the sinusoidal signal and amplify the energy output, (2) high voltage circuit to transform the low primary voltage to a high secondary voltage, and (3) design of the sample holder between the high voltage capacitor plates.

Figure 2: (Top) Illustration of the snow heating device. The setup includes a function generator, an audio amplifier and a plastic box with all the high voltage parts. The lid of the box is secured by a safety switch. (Bottom) An illustration of the inner part of the box is shown. It illustrates the high voltage parts with the 60 mm capacitor. Additionally, the CT sample holder with the 34 mm capacitor is shown.

Figure 3: Typical measured temperature T(t), current I_{RMS}(t), voltage U_{RMS}(t), and phase shift φ(t) profile of a heating process for snow density of (a) 438 kg m^{-3}, (b) 539 kg m^{-3}, (c) 612 kg m^{-3}, and (d) 917 kg m^{-3}.

Figure 4: Typical measured temperature T(t), impedance R_{RMS}(t) and power P_{RMS}(t), profile of a heating process for snow density of (a) 438 kg m^{-3}, (b) 539 kg m^{-3}, (c) 612 kg m^{-3}, and (d) 917 kg m^{-3}.

Figure 5: Heating efficiency and the complex dielectric constant of dry snow at T = 0 °C for various snow sample.

Figure 6: The temporal evolution of the liquid water mass and volume fraction based on the measured power for snow density of (a) 438 kg m^{-3}, (b) 539 kg m^{-3}, (c) 612 kg m^{-3}, and (d) 917 kg m^{-3}.

Figure 7: 3D micro-computer tomography (CT) picture to visualize the water content in snow after water percolation. The scanned image has a volume of 200 x 200 x 20 voxels (3.6 mm x 3.6mm x 0.36mm). Blue indicates the ice structure and orange shows the water part.

Figure 8: Photography under the microscope to illustrate the liquid water content in the wet snow sample: (left) snow structure of snow before the experimental run, (right) the same snow sample after 2 hours with an estimated liquid-water content of 12 wt%.

https://doi.org/10.5194/tc-2020-56
Preprint. Discussion started: 3 May 2020

The Cryosphere Discussions
Open Access
EGU

Figure 9: Dividing the heating process in three different processes: (1) dry snow heating process up to 0 °C indicating a temperature and snow structure dependency on the measured values; (2) wet snow heating at stagnating temperature of 0°C and the presence of uniformed distributed liquid water changes the dielectric properties of the snow sample; and (3) starting point of water percolation in the snow sample introducing an inhomogeneous mixture where liquid water treasures up at the bottom of the sample holder and is leaving bigger pores in the upper part.

Figure 10: Visualization of water percolation after an experimental run. The sample holder was aligned vertically between the capacitor plates. Water percolated in the upper part of the sample and accumulated at the bottom of the sample holder leading to an inhomogeneous mixture of the sample affecting the heating process of the sample.

https://doi.org/10.5194/tc-2020-56
Preprint. Discussion started: 3 May 2020

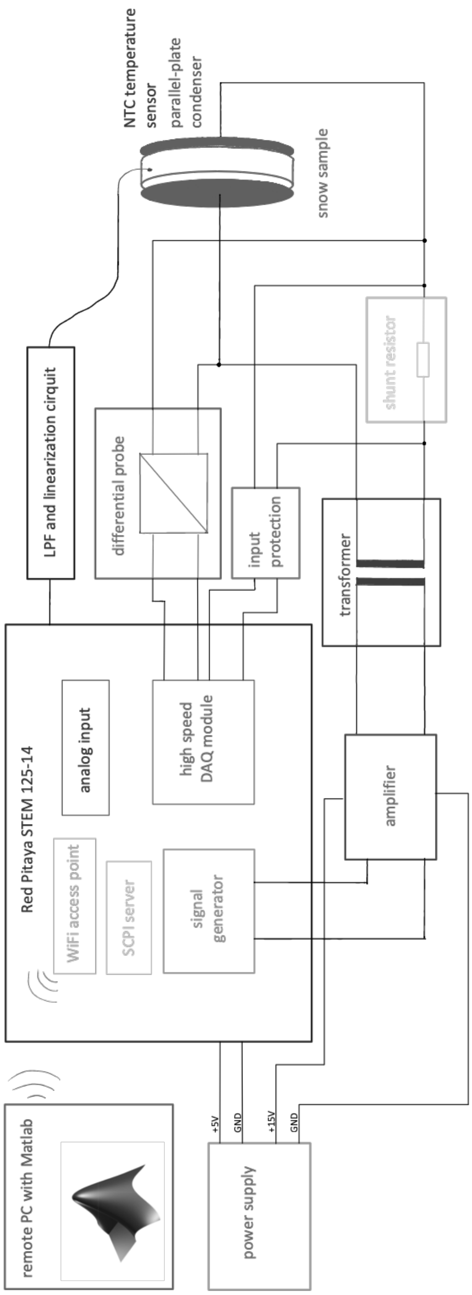

Figure 1

https://doi.org/10.5194/tc-2020-56
Preprint. Discussion started: 3 May 2020

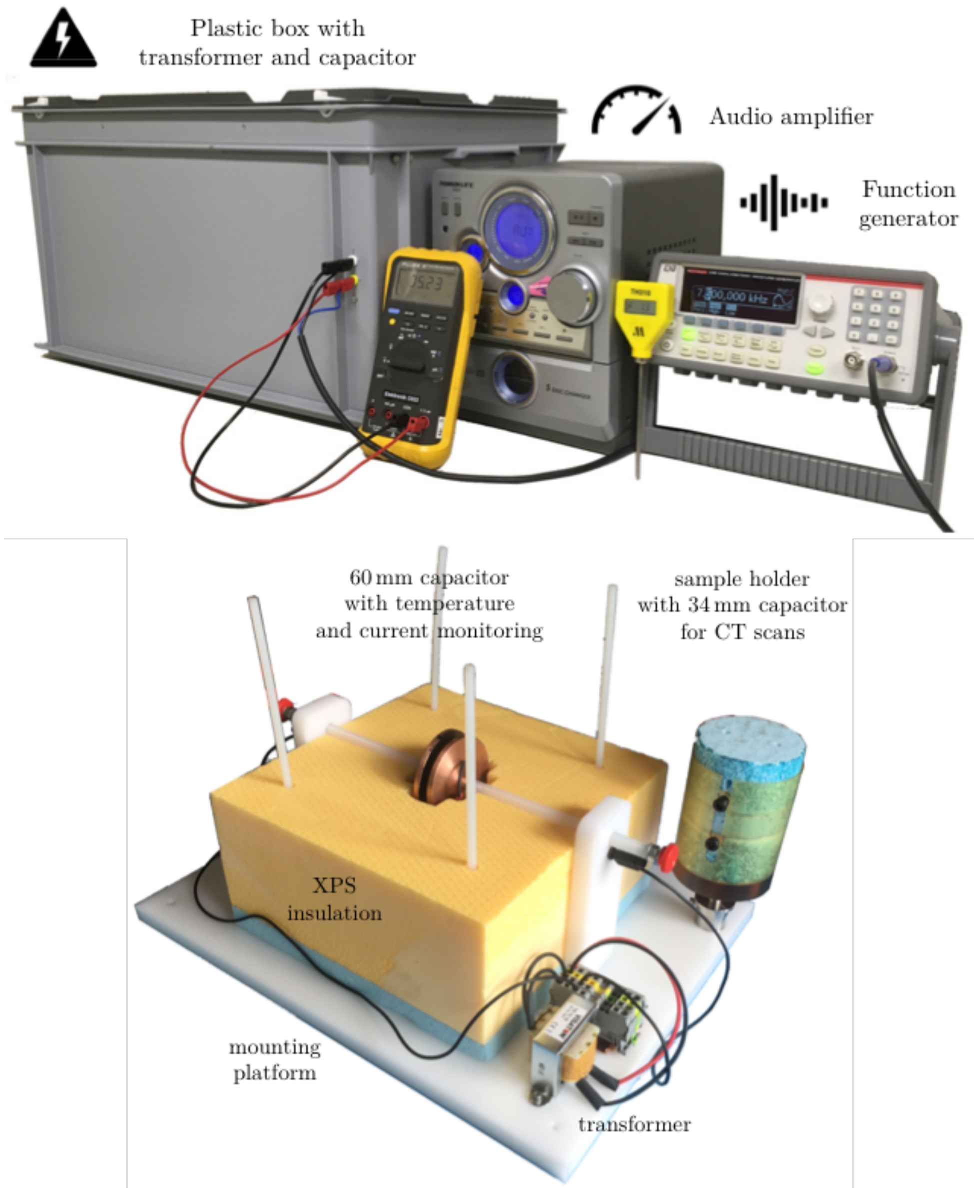

Figure 2

https://doi.org/10.5194/tc-2020-56
Preprint. Discussion started: 3 May 2020

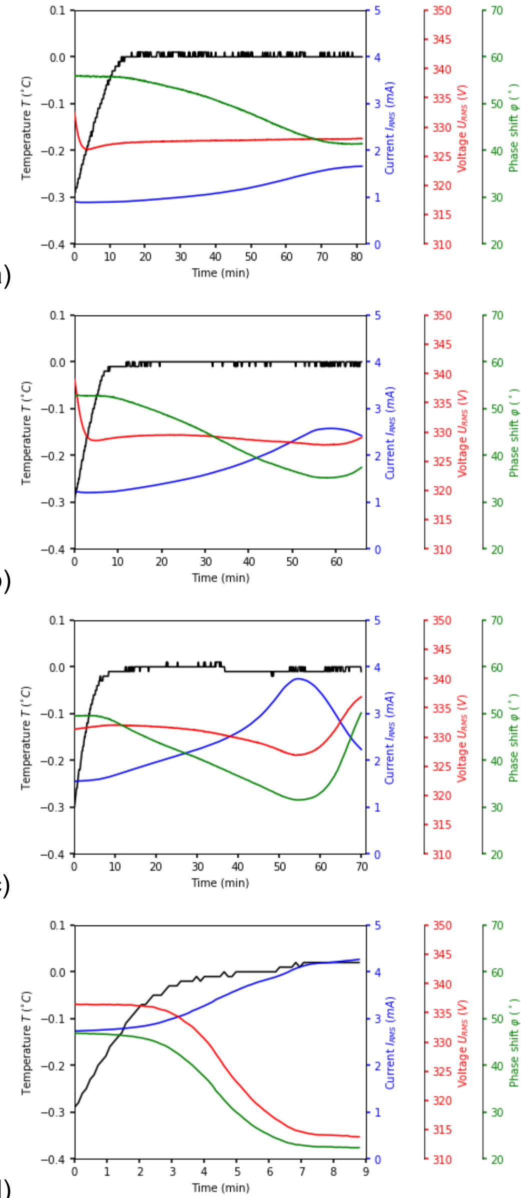

a) b) c) d)

Figure 3

https://doi.org/10.5194/tc-2020-56
Preprint. Discussion started: 3 May 2020

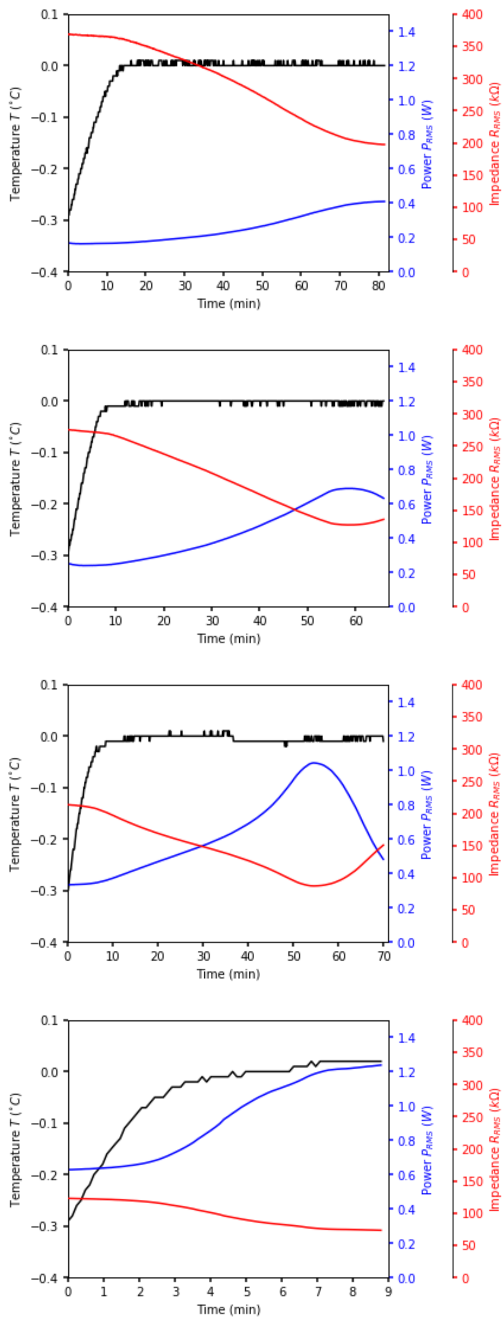

a)

b)

c)

d)

Figure 4

https://doi.org/10.5194/tc-2020-56
Preprint. Discussion started: 3 May 2020

The Cryosphere Discussions
Open Access
EGU

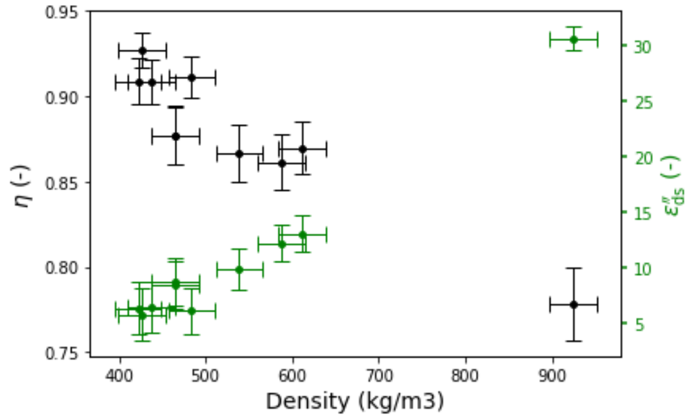

Figure 5

https://doi.org/10.5194/tc-2020-56
Preprint. Discussion started: 3 May 2020

The Cryosphere
Discussions
Open Access

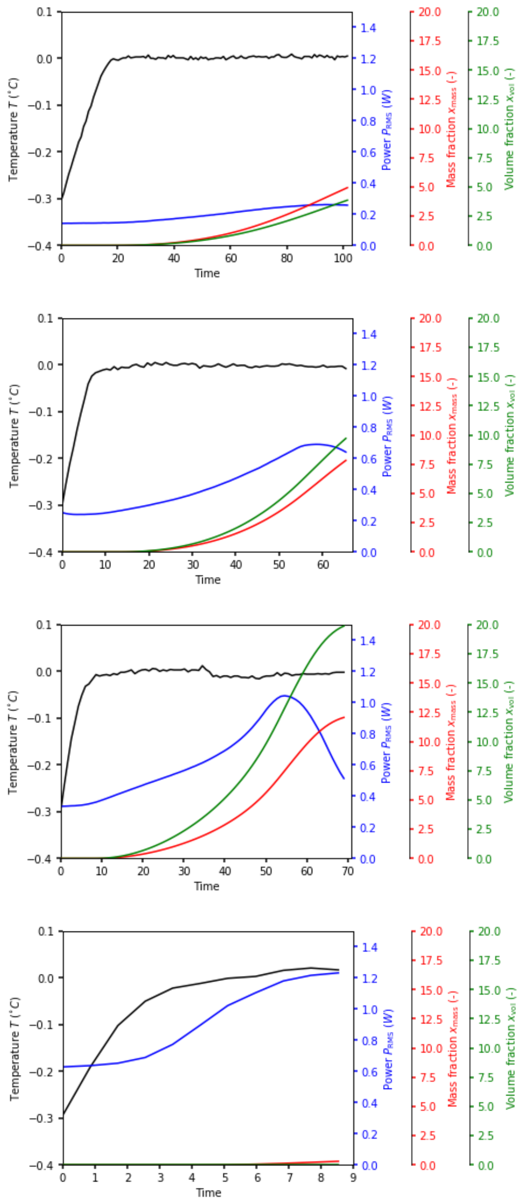

a)

b)

c)

d)

Figure 6

https://doi.org/10.5194/tc-2020-56
Preprint. Discussion started: 3 May 2020

The Cryosphere Discussions
Open Access
EGU

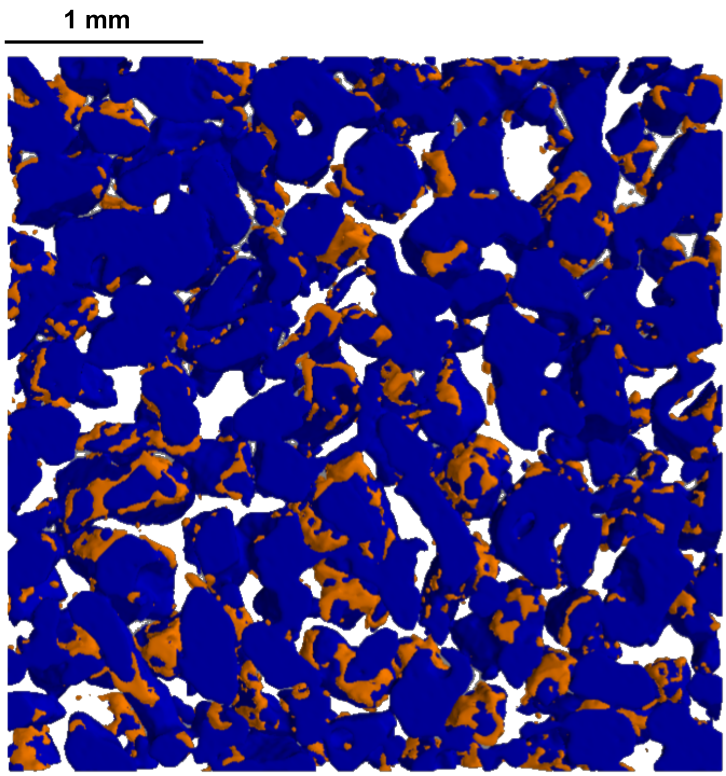

Figure 7

https://doi.org/10.5194/tc-2020-56
Preprint. Discussion started: 3 May 2020

The Cryosphere Discussions
Open Access

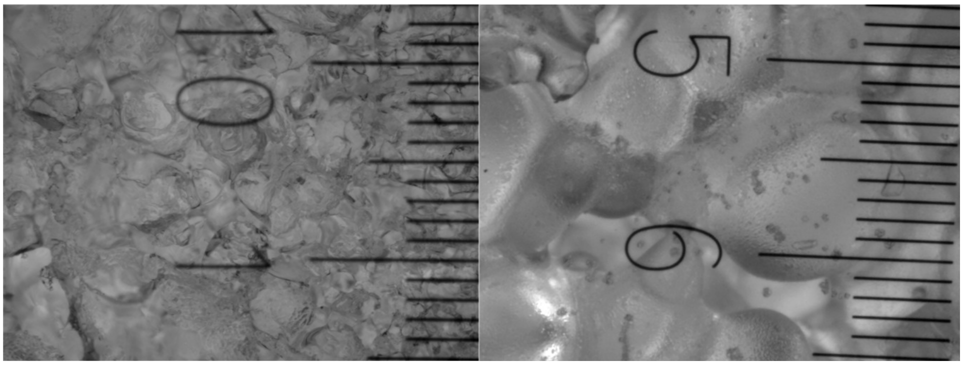

Figure 8

https://doi.org/10.5194/tc-2020-56
Preprint. Discussion started: 3 May 2020

The Cryosphere
Discussions
Open Access

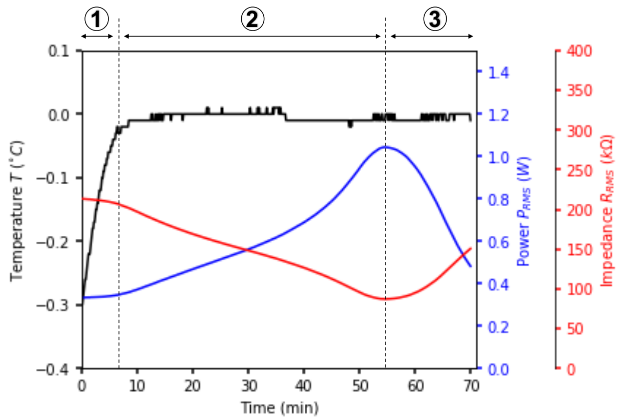

Figure 9

https://doi.org/10.5194/tc-2020-56
Preprint. Discussion started: 3 May 2020

The Cryosphere
Discussions
Open Access

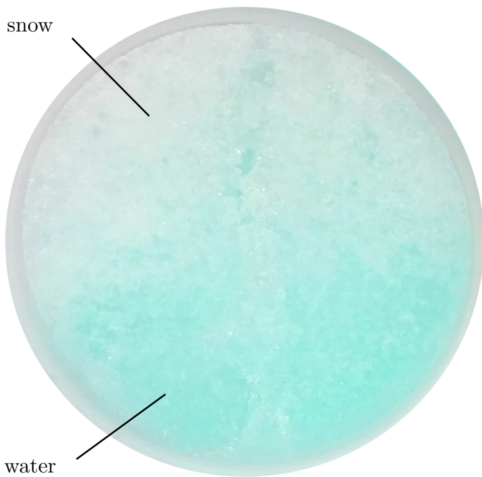

631
632
633 Figure 10